Bound Peptide-Dependent Thermal Stability of Major Histocompatibility Complex Class II Molecule I-E^{k†}

Keigo Saito,[‡,§] Masayuki Oda,[§,||] Akinori Sarai,[⊥] Takachika Azuma,[‡] and Haruo Kozono*[,‡]

Research Institute for Biological Sciences, Tokyo University of Science, 2669, Yamazaki, Noda, Chiba 278-0022, Japan, Graduate School of Agriculture, Kyoto Prefectural University, 1-5, Shimogamo Nakaragi-cho, Sakyo-ku, Kyoto 606-8522, Japan, and Faculty of Computer Science and System Engineering, Kyushu Institute of Technology, 680-4, Kawazu, Iizuka, Fukuoka 820-8502, Japan

Received January 22, 2004; Revised Manuscript Received June 8, 2004

ABSTRACT: We used differential scanning calorimetry to study the thermal denaturation of murine major histocompatibility complex class II, I-E^k, accommodating hemoglobin (Hb) peptide mutants possessing a single amino acid substitution of the chemically conserved amino acids buried in the I-E^k pocket (positions 71 and 73) and exposed to the solvent (position 72). All of the I-E^k-Hb(mut) molecules exhibited greater thermal stability at pH 5.5 than at pH 7.4, as for the I-E^k-Hb(wt) molecule, which can explain the peptide exchange function of MHC II. The thermal stability was strongly dependent on the bound peptide sequences; the I-E^k-Hb(mut) molecules were less stable than the I-E^k-Hb(wt) molecules, in good correlation with the relative affinity of each peptide for I-E^k. This supports the notion that the bound peptide is part of the completely folded MHC II molecule. The thermodynamic parameters for I-E^k-Hb(mut) folding can explain the thermodynamic origin of the stability difference, in correlation with the crystal structural analysis, and the limited contributions of the residues to the overall conformation of the I-E^k−peptide complex. We found a linear relationship between the denaturation temperature and the calorimetric enthalpy change. Thus, although the MHC II−peptide complex could have a diverse thermal stability spectrum, depending on the amino acid sequences of the bound peptides, the conformational perturbations are limited. The variations in the MHC II−peptide complex stability would function in antigen recognition by the T cell receptor by affecting the stability of the MHC II−peptide−T cell receptor ternary complex.

Major histocompatibility complex class II (MHC II)[1] is expressed on antigen-presenting cells and presents exogenous peptides to CD4 T cells (*1*). MHC molecules can bind various peptides, which are derived from either foreign or self proteins (*2*, *3*). T cell activation results from T cell receptor (TCR) recognition of an immunogenic peptide associated with MHC II. The murine MHC II, I-E^k, in complexes with the peptide encompassing positions 64−76 of the d allele of mouse hemoglobin (Hb) and its amino acid-substituted Hb peptides, has been studied systemically as a model system for T cell activation (*4*). The amino acid-substituted peptides, called altered peptide ligands (APLs), can modify the T cell activation level; that is, some APLs partially or fully activate T cells (partial or full agonists), and others inhibit their activation (antagonists) (*4*−*6*).

The crystal structures of MHC II−peptide complexes (pMHC II) have shown that the peptide binding specificity is relevant to the interactions between the MHC II pockets, designated P1, P4, P6, and P9, and the corresponding peptide anchor residues. The I-E^k-Hb crystal structures revealed the respective characteristics of the four I-E^k molecule pockets (*7*−*9*). P1 can accept aliphatic and hydrophobic side chains. P4 is large and hydrophobic. P6 is very hydrophilic. P9 is a long, negatively charged tunnel. Although alignments of bound peptides with I-E^k showed the existence of preferred amino acid residues, which fit into the respective pockets, the anchor residues were not limited to a particular residue (*9*, *10*). Thus, we can imagine that each pocket interaction is somewhat flexible. However, it is worth noting that conservative mutations on the Hb peptide bound to I-E^k, such as the substitution of Tyr for Phe at P4 (F71Y) and that of Asp for Glu at P6 (E73D), can alter the T cell activation properties (*5*, *6*).

One of the APLs, E73D, has been classified as a weak agonist or antagonist (*11*). With this substitution, the peptide's affinity for I-E^k is slightly decreased, while the T cell activation is significantly affected (*6*). This is interesting because the P6 anchor residue was shown to be the MHC

† This work was supported by grants to H.K. from the Ministry of Education, Culture, Science and Sports of Japan.

* To whom correspondence should be addressed: Research Institute for Biological Sciences, Tokyo University of Science, 2669, Yamazaki, Noda, Chiba 278-0022, Japan. E-mail: kozonoh@rs.noda.tus.ac.jp. Telephone: +81-4-7121-4083. Fax: +81-4-7121-4089.

‡ Tokyo University of Science.

§ These authors contributed equally to this work.

|| Kyoto Prefectural University.

⊥ Kyushu Institute of Technology.

[1] Abbreviations: MHC II, major histocompatibility complex class II; TCR, T cell receptor; Hb, peptide encompassing residues 64−76 of the mouse hemoglobin d allele; I-E^k-Hb(wt), I-E^k bound to the Hb wild-type peptide; I-E^k-Hb(mut), I-E^k bound to a Hb mutant peptide; APL, altered peptide ligand; pMHC II, MHC II−peptide complex; DSC, differential scanning calorimetry; T_d, denaturation temperature; ΔH_{cal}, calorimetric enthalpy change; ΔH_{vH}, van't Hoff enthalpy change; ΔT_d, difference in the T_d value of I-E^k-Hb(mut) relative to that of I-E^k-Hb(wt); ΔC_p, molar excess heat capacity change.

10.1021/bi049838f CCC: $27.50
Published on Web 07/16/2004

contact site, not the TCR contact site. The I-E^k-Hb(E73D) and I-E^k-Hb(wt) crystal structures revealed no significant variations in the I-E^k-Hb molecule itself, while the relative orientation of the peptide P5−P8 main chain was altered (*7*, *8*). To date, the different TCR binding kinetics, and especially the dissociation rate of the interaction, caused by this substitution have been considered to be important in T cell signaling (*11*, *12*). In general, new insights into these subtle differences leading to different responses, which are not revealed by static structural analyses, can be provided by dynamic structural analyses, such as binding kinetics and thermodynamics (*13*, *14*).

In this study, the thermodynamic properties of I-E^k in complex with Hb mutant peptides were characterized by using differential scanning calorimetry (DSC), to analyze the effects of conservative mutations of the bound peptide on the dynamic structure of pMHC II. In addition to the I-E^k-Hb(E73D), we prepared I-E^k-Hb(F71Y) and I-E^k-Hb(N72Q). Residue 71 is the P4 anchor residue, and the F71Y mutation greatly affected the peptide's affinity for I-E^k (*6*). In contrast to residues 71 and 73, which face the MHC binding surface, residue 72 is on the TCR contact site, and a mutational study revealed that this residue primarily affects T cell activation (*11*). The N72Q mutation caused no responses in isolated T cells, although it did not affect the affinity for I-E^k (*6*).

We recently reported the increased thermodynamic stability of I-E^k-Hb(wt) at an acidic pH, which provided new information about the dynamic conformational change as a function of pH, to explain the peptide exchange mechanism (*14*). Thermodynamic parameters, such as the enthalpy change (ΔH) and the entropy change (ΔS), in addition to the denaturation temperature (T_d), are good indicators for detecting subtle conformational differences in flexible proteins, such as MHC molecules. Although the thermal denaturation of I-E^k-Hb(wt) was irreversible, the thermodynamic parameters were analyzed as an equilibrium quantity, because a large activation energy was observed (*14*, *15*). We now report the contribution of a bound peptide to the thermodynamic stability of I-E^k-Hb at pH 5.5 and 7.4, and discuss the correlation between the peptide-dependent conformational differences and the biological function, mediated by TCR recognition. In addition, using I-E^k-Hb(E73D), the crystal structure of which was determined, the pH-dependent thermal stability was precisely analyzed. These data support the previous conclusion that the conformation at a mildly acidic pH differs from that at a neutral pH, which facilitates peptide exchange.

MATERIALS AND METHODS

Construction of Baculovirus Transfer Vectors and Production of Soluble I-E^k-Hb Molecules. Site-directed mutations were introduced by PCR, with splicing by the overlap extension method (*16*, *17*). The amplified mutated DNA, encoding Hb mutants covalently linked with the I-E^k β chain gene, was inserted into the pBACpH10pH transfer vector using TAKARA Ligation Kit II (TAKARA). The recombinant transfer vector was cotransfected with linearized baculovirus genomic DNA into SF9 insect cells for the production of the recombinant virus (Pharmingen). The recombinant viruses were cloned by the limiting dilution method and amplified by infection. Soluble I-E^k-Hb molecules, produced by the baculovirus-infected SF9 insect cells, were purified by immunoaffinity column chromatography with 14-4-4S, a monoclonal anti-MHC II antibody, followed by gel filtration chromatography, as described previously (*14*).

Gel Filtration Chromatography. Gel filtration chromatography was performed with an HPLC system, using a Superdex 200 column (Amersham Biosciences) in 10 mM Tris-HCl (pH 7.4) containing 150 mM NaCl and 1 mM EDTA. The flow speed was 0.5 or 1.0 mL/min, and the elution profiles were recorded at 280 nm using a UV detector.

DSC Measurements. DSC experiments were carried out on a Microcal MCS calorimeter. Samples were prepared in 10 mM phosphate buffer with 150 mM NaCl, adjusted to an appropriate pH between 5.0 and 8.0. Data were collected in the temperature range between 25 and 90 °C, at a heating rate of 1.0 °C/min. The data analyses were performed with the DSC analysis software Microcal Origin, version 4.1. The calorimetric enthalpy change (ΔH_{cal}) was determined by integrating the area in each heat capacity curve. The van't Hoff enthalpy change (ΔH_{vH}), assuming the two-state transition, was calculated by the following equation:

$$\Delta H_{vH}(T_d) = 4RT_d^2 \frac{C_p(T_d)}{\Delta H_{cal}(T_d)} \quad (1)$$

where C_p is the molar excess heat capacity and R is the gas constant. The Gibbs free energy of unfolding as a function of temperature, $\Delta G_d(T)$, could be calculated from the following equation:

$$\Delta G_d(T) = \Delta H_{cal}(T_d)\left(1 - \frac{T}{T_d}\right) - \Delta C_p T \ln \frac{T}{T_d} - \Delta C_p(T_d - T) \quad (2)$$

RESULTS

Gel Filtration Analysis of I-E^k-Hb Mutant Molecules. The eluate of the immunoaffinity column chromatography, containing the I-E^k-Hb molecules, was fractionated by gel filtration HPLC. The profiles differed, depending on the peptide type (Figure 1a). Most fractions of I-E^k without the peptide were high-molecular weight aggregates, which made it difficult to purify the I-E^k molecule itself. The profile of I-E^k-Hb(F71Y) exhibited some size heterogeneity, including the $\alpha\beta$ heterodimer and aggregates, while the profiles of I-E^k-Hb(N72Q) and I-E^k-Hb(E73D) were similar to that of I-E^k-Hb(wt). Each of the purified proteins, including I-E^k-Hb(F71Y), ran as a single peak on gel filtration rechromatography (Figure 1b), indicating that these soluble proteins form the correct $\alpha\beta$ heterodimer.

Thermal Stability of I-E^k-Hb Mutant Molecules at pH 7.4 and 5.5. DSC measurements of three I-E^k molecules complexed with Hb mutant peptides, I-E^k-Hb(F71Y), I-E^k-Hb(N72Q), and I-E^k-Hb(E73D), were carried out at pH 7.4 and 5.5. These two pH values were chosen because of their importance for the function of MHC II, i.e., peptide binding and antigen presentation. The molar excess heat capacity curves are shown in Figure 2, in which the data for I-E^k-Hb(wt) were included for comparison. Like I-E^k-Hb(wt), I-E^k-Hb(mut) underwent irreversible unfolding, as shown by the lack of reproduced excess heat capacity in the second scanning (*14*). All of the curves in the first scan showed

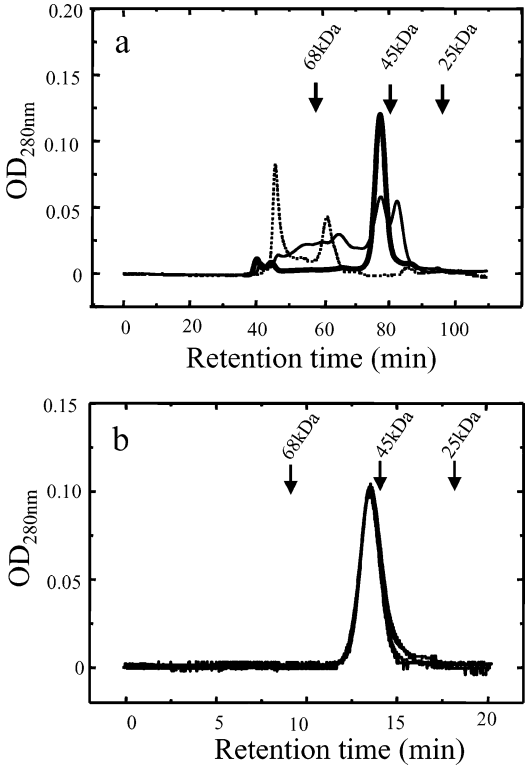

FIGURE 1: Gel filtration HPLC of I-E^k-Hb molecules. (a) The eluate of the immunoaffinity column chromatography, containing I-E^k-Hb molecules, was loaded onto a Superdex 200 column (16 mm × 60 cm). Chromatograms of I-E^k-Hb(wt), I-E^k-empty, and I-E^k-Hb(F71Y) are shown with thick, dotted, and thin lines, respectively. The flow rate was 1 mL/min. (b) The purified solution of I-E^k-Hb molecules was loaded onto a Superdex 200 column (10 mm × 30 cm). The flow rate was 0.5 mL/min. The retention times of standard proteins used to calibrate the column, bovine serum albumin (68 kDa), hen egg albumin (45 kDa), and chymotrypsinogen A (25 kDa), are also given.

small transition ranges of ~10 °C, indicating the high cooperativity of this transition. The irreversible transition at a heating rate of 1.0 °C/min should be followed by the dissociation of each subunit and its denaturation after the partial unfolding of the peptide from MHC II (*14*). Therefore, the thermodynamic parameters for denaturation of I-E^k-Hb(mut) were determined as the equilibrium, assuming the two-state transition, like those of I-E^k-Hb(wt) (Table 1). For all of the I-E^k-Hb(mut) molecules, the thermal stability at the acidic pH was higher than that at the neutral pH. The difference in the T_d values relative to that of I-E^k-Hb(wt) (ΔT_d) at the acidic pH was smaller than that at the neutral pH.

Table 1: Thermodynamic Parameters for Denaturation of I-E^k-Hb(wt), I-E^k-Hb(F71Y), I-E^k-Hb(N72Q), and I-E^k-Hb(E73D) at pH 7.4 and 5.5

pMHC II	concn (mM)	T_d (°C)	ΔH_{cal} (kJ/mol)	ΔH_{vH} (kJ/mol)	$\Delta H_{cal}/\Delta H_{vH}$
		pH 7.4			
I-E^k-Hb(wt)[a]	0.0069	67.2	744	600	1.2
I-E^k-Hb(wt)[a]	0.0037	65.9	756	593	1.3
I-E^k-Hb(wt)[a]	0.0017	66.9	744	608	1.2
I-E^k-Hb(wt)[b]		66.7 ± 0.8	748 ± 8	600 ± 8	1.2
I-E^k-Hb(F71Y)	0.0102	56.6	264	555	0.5
I-E^k-Hb(N72Q)	0.0085	64.6	638	593	1.1
I-E^k-Hb(E73D)	0.0068	62.4	567	615	0.9
I-E^k-Hb(E73D)	0.0098	60.9	522	528	1.0
I-E^k-Hb(E73D)[b]		61.7 ± 0.8	545 ± 23	572 ± 44	1.0
		pH 5.5			
I-E^k-Hb(wt)[a]	0.0069	75.4	723	702	1.0
I-E^k-Hb(F71Y)	0.0059	68.7	362	724	0.5
I-E^k-Hb(N72Q)	0.0050	74.5	694	698	1.0
I-E^k-Hb(E73D)	0.0049	72.2	688	675	1.0
I-E^k-Hb(E73D)	0.0089	71.1	632	620	1.0
I-E^k-Hb(E73D)[b]		71.7 ± 0.6	660 ± 28	648 ± 28	1.0

[a] Data were taken from ref *14*. [b] Averaged values.

The stability of I-E^k-Hb(F71Y) was the lowest among the three I-E^k-Hb(mut) molecules used in this study. The ΔH_{cal} value of I-E^k-Hb(F71Y) was much smaller than those of the others, and the $\Delta H_{cal}/\Delta H_{vH}$ ratio was 0.5, while those of the other I-E^k-Hb(mut) molecules were around 1.0. Both the T_d and ΔH_{cal} values of I-E^k-Hb(N72Q) were slightly lower than those of I-E^k-Hb(wt), although the substitution site is opposite to the MHC binding surface. The stability of I-E^k-Hb(E73D) was also lower than that of I-E^k-Hb(wt). An enhanced thermodynamic analysis of this pMHC II complex was carried out to elucidate the pH-dependent conformational and energetic properties, as described below.

Thermal Denaturation Analysis of I-E^k-Hb(E73D) as a Function of pH. The excess heat capacity curves for I-E^k-Hb(E73D) as a function of pH are shown in Figure 3a, and the thermodynamic parameters are summarized in Table 2. While both the T_d and ΔH_{cal} values were lower than those of I-E^k-Hb(wt), the stability at the mildly acidic pH was higher than that at the neutral pH. The correlation between T_d and ΔH_{cal} seems to be classified into two groups, one for the acidic pH and the other for the neutral pH (Figure 3b),

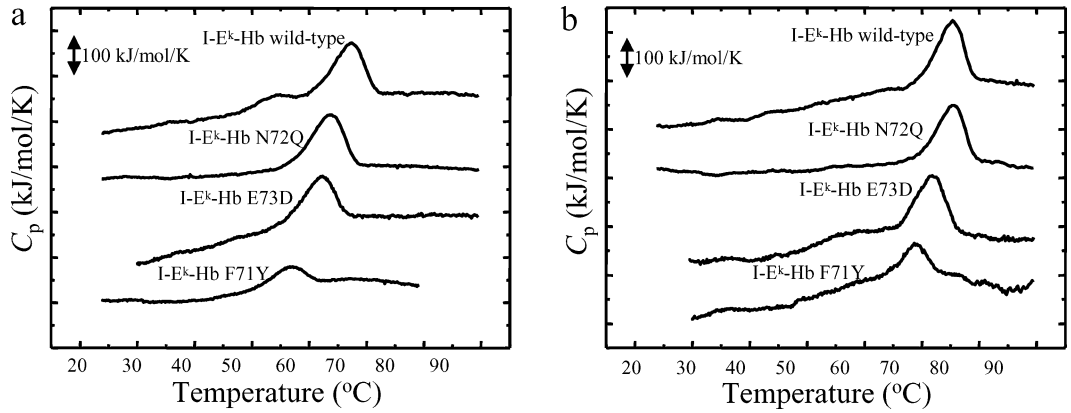

FIGURE 2: Typical excess heat capacity curves of I-E^k-Hb(wt), I-E^k-Hb(F71Y), I-E^k-Hb(N72Q), and I-E^k-Hb(E73D) at pH 7.4 (a) and pH 5.5 (b). The temperature was increased by 1.0 °C/min. The protein concentration for the measurement was approximately 0.4 mg/mL. Data for I-E^k-Hb(wt) were taken from ref *14*.

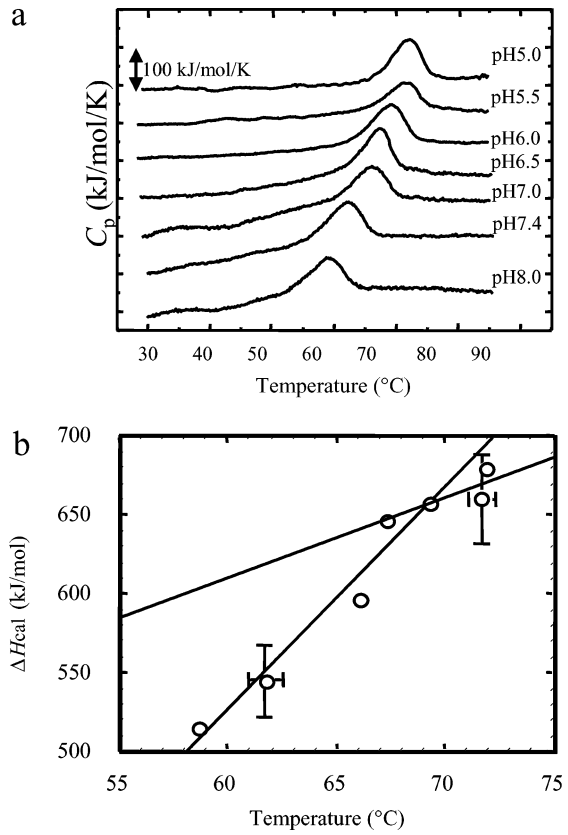

FIGURE 3: Thermodynamic profiles of I-E^k-Hb(E73D) as a function of pH. (a) Typical excess heat capacity curves. The temperature was increased by 1.0 °C/min. (b) Correlation between T_d and ΔH_{cal}. The slopes were determined by the linear least-squares method.

Table 2: Thermodynamic Parameters for Denaturation of I-E^k-Hb(E73D) as a Function of pH

pH	concn (mM)	T_d (°C)	ΔH_{cal} (kJ/mol)	ΔH_{vH} (kJ/mol)	$\Delta H_{cal}/\Delta H_{vH}$
5.0	0.0122	71.9	679	634	1.1
5.5[a]	0.0049	72.2	688	675	1.0
5.5[a]	0.0089	71.1	632	620	1.0
6.0	0.0117	69.3	658	620	1.1
6.5	0.0066	67.3	646	681	1.0
7.0	0.0063	66.1	597	585	1.0
7.4[a]	0.0068	62.4	567	615	0.9
7.4[a]	0.0098	60.9	522	528	1.0
8.0	0.0063	58.7	515	605	0.9

[a] Data were taken from Table 1.

as observed for I-E^k-Hb(wt) (*14*). This indicates that the pH-dependent change in stability is a unique property of MHC II and is independent of bound peptides, which is consistent with the results from previous structural and functional analyses of pMHC II. The molar excess heat capacity changes (ΔC_p) determined from this correlation are 5.0 kJ mol^{-1} K^{-1} for the mildly acidic pH and 14.1 kJ mol^{-1} K^{-1} for the neutral pH.

DISCUSSION

In this report, we address the question of how bound peptides energetically contribute to pMHC II stability and attempt to detect the subtle conformational change caused by APLs, which is critical for TCR recognition. Considering the fact that the bound peptides participate in the complete folding of the MHC molecule (*18*, *19*), an amino acid substitution within a peptide would affect the folding of pMHC II. This is supported by the finding that the order of the T_d values of I-E^k-Hb(wt) and I-E^k-Hb(mut) follows that of the affinity of each peptide for I-E^k, except for I-E^k-Hb(N72Q): I-E^k-Hb(wt) = I-E^k-Hb(N72Q) > I-E^k-Hb(E73D) > I-E^k-Hb(F71Y) (*6*). The results of gel filtration HPLC for the purification of each I-E^k-Hb molecule also displayed different properties (Figure 1a), in good correlation with the thermal stability. The aggregation of I-E^k without the peptide would be due to misfolding, and the heterogeneous profile of the least stable pMHC II in this study, I-E^k-Hb(F71Y), would be due to its stability midway between complete folding and misfolding. It should also be noted that purified I-E^k-Hb(F71Y) exhibited a single peak during rechromatography, corresponding to the $\alpha\beta$ heterodimer, similar to the other two I-E^k-Hb(mut) and I-E^k-Hb(wt) molecules (Figure 1b). This indicates that correct peptide binding with sufficient binding affinity and/or kinetics can stabilize the pMHC II molecule at a physiological temperature.

In addition to its unique profile from gel filtration HPLC, the $\Delta H_{cal}/\Delta H_{vH}$ value of I-E^k-Hb(F71Y) differed from the values for I-E^k-Hb(N72Q), I-E^k-Hb(E73D), and I-E^k-Hb(wt). As discussed previously, the thermal denaturation process of I-E^k-Hb should contain several transitions (*14*). The smaller $\Delta H_{cal}/\Delta H_{vH}$ value indicates that the first transition, which may be the partial unfolding of the peptide from MHC II, accelerates the following transitions, resulting in a somewhat cooperative transition without intermediate states. The binding affinity and/or kinetics of the bound peptide may influence the dynamic properties of pMHC II.

In the analysis of the pH-dependent thermal stability of I-E^k-Hb(E73D), the correlation of ΔH_{cal} with T_d indicated that the folding of this pMHC II at the mildly acidic pH differs from that at the neutral pH, as observed in I-E^k-Hb(wt) (*14*). This suggests that the pH-dependent properties of the I-E^k-Hb molecule are preserved, and the effects of the peptide difference are limited to subtle and local conformations. The similar pH dependency and ΔC_p values for I-E^k-Hb(E73D) and I-E^k-Hb(wt) are consistent with the crystal structure analysis, which did not reveal notable structural differences in the I-E^k molecules (*8*). In general, the pH-dependent thermodynamics of I-E^k-Hb can arise from both the structural effects and the proton-linked effects (*20*, *21*). Although these thermodynamic results were obtained in phosphate buffer, which has a lower enthalpy change for the deprotonation, the groups in proteins that are titrating in the neutral-to-basic pH range will have large ionization enthalpies themselves, and the difference in the ionization enthalpies between the native and denatured states may contribute to the pK_a shifts and cause a significant pH dependence. We examined the proton-linked effects on I-E^k-Hb(wt) by using MOPS buffer, and the result suggested that the proton-linked effects were responsible for the pH dependence to some extent (*14*). If we assume that the pH-dependent properties of I-E^k-Hb(E73D) are similar to those of I-E^k-Hb(wt), the conformational enthalpy change of I-E^k-Hb(E73D) would be slightly lower than the experimentally determined ΔH_{cal} values.

If we assume that the ΔC_p values of I-E^k-Hb(mut) used in this study were similar to those of I-E^k-Hb(wt), it is possible to calculate the thermodynamic parameters at the reference temperature in an effort to analyze the thermody-

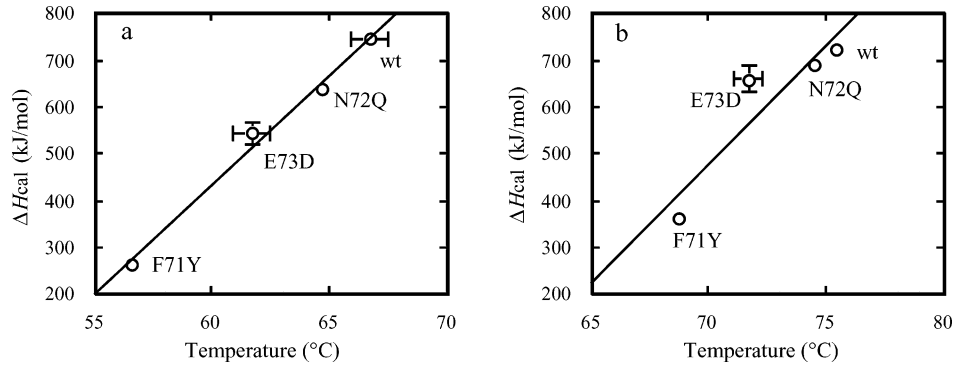

FIGURE 4: Correlation between T_d and ΔH_{cal} of I-E^k-Hb(wt), I-E^k-Hb(F71Y), I-E^k-Hb(N72Q), and I-E^k-Hb(E73D) at pH 7.4 (a) and pH 5.5 (b). The T_d and ΔH_{cal} values were taken from Table 1. The slopes were determined by the linear least-squares method, and the correlation coefficients were 0.99 for pH 7.4 and 0.92 for pH 5.5.

Table 3: Thermodynamic Parameters for Denaturation of I-E^k-Hb(wt), I-E^k-Hb(F71Y), I-E^k-Hb(N72Q), and I-E^k-Hb(E73D) at 75.4 °C

pMHC	T_d[a] (°C)	ΔT_d (°C)	ΔH (kJ/mol)	$T\Delta S$ (kJ/mol)	ΔG (kJ/mol)
		pH 7.4			
I-E^k-Hb(wt)[b]	66.7	−8.7	886	907	−21
I-E^k-Hb(F71Y)[c]	56.6	−18.8	563	586	−23
I-E^k-Hb(N72Q)[c]	64.6	−10.8	810	833	−23
I-E^k-Hb(E73D)[b,c]	61.7	−13.7	763	789	−26
I-E^k-Hb(E73D)[b,d]			738	764	−26
		pH 5.5			
I-E^k-Hb(wt)	75.4		723	723	0
I-E^k-Hb(F71Y)[c]	68.7	−6.7	436	444	−7.8
I-E^k-Hb(N72Q)[c]	74.5	−0.9	704	706	−1.8
I-E^k-Hb(E73D)[b,c]	71.7	−3.7	701	708	−7.3
I-E^k-Hb(E73D)[b,d]			679	686	−7.2

[a] Data were taken from Table 1. [b] The averaged T_d and ΔH values in Table 1 were used to calculate these values. [c] Calculated using the ΔC_p values of I-E^k-Hb(wt) (*14*). [d] Calculated using the ΔC_p values of I-E^k-Hb(E73D), obtained in this study.

namic origin of the stability difference (Table 3). The increased stability at the mildly acidic pH for all of the I-E^k-Hb(mut) molecules was due to the decreased ΔS value, as for I-E^k-Hb(wt), even though the conformational ΔH values at the acidic pH are somewhat lower than the experimentally determined ΔH_{cal} values. This supports the notion that the native structure of I-E^k-Hb at the mildly acidic pH is more flexible, which can facilitate the peptide exchange, and subtle differences in the bound peptide do not alter the overall character. The smaller difference in the ΔT_d values at the acidic pH relative to those at the neutral pH may support the flexible nature of MHC II at the acidic pH; that is, the effects of mutations may be absorbed within the more flexible conformation.

The conservative substitution at position 71 reduced the stability of I-E^k-Hb(F71Y), with a relatively large decrease in ΔH (Table 1). This can be explained by the polar hydroxyl group of Tyr71 in the hydrophobic P4 environment, and its steric hindrance, which was indicated in the I-E^k-Hb(wt) crystal structure (*7*). Since residue 72 of the Hb peptide protrudes toward the surrounding water, the slightly lower stability of I-E^k-Hb(N72Q) would be due to the different hydrophobicities of Asn and Gln (*22*, *23*). The Asn side chain is critical for T cell activation, because of its direct contact with TCR (*11*). In contrast, the substitution of Asp for Glu at position 73 should indirectly affect the TCR recognition. The I-E^k-Hb(E73D) crystal structure revealed that the structural difference from the I-E^k-Hb(wt) exists in the peptide main chain around the substituted site, in residues P5−P8, not in I-E^k itself (*7*, *8*). The different relative orientation of the peptide should reduce its binding affinity and decrease the overall stability. The crystal structure of I-E^k-Hb(E73D) also revealed that water molecules play a critical role in forming new hydrogen bonds between I-E^k and the E73D peptide (*8*). The increased ΔS values for the I-E^k-Hb(E73D) denaturation at the mildly acidic pH, relative to those of I-E^k-Hb(wt), may be due to the dehydration effect (Tables 1 and 2). The fact that the increased ΔS values were not observed at the neutral pH implies that the hydrogen bonds involving water molecules are specific to the peptide recognition at an acidic pH. In the P6 pocket, the hydrogen bonding cluster of carboxylate groups could be disrupted at a neutral pH, due to their unusual pK_a values (*24*, *25*).

A linear relationship existed between the ΔH_{cal} and T_d values for all of the I-E^k-Hb molecules used in this study (Figure 4). This relationship can also be applied to other I-E^k−peptide complexes, such as the I-E^k complex with moth cytochrome *c* peptide 82−103, which is more stable than I-E^k-Hb(wt) (unpublished results). This indicates that various peptides probably affect the thermal stability with similar degrees of conformational perturbation, thus maintaining a linear relationship between the ΔH_{cal} and T_d values.

The inherent property of MHC II is its versatility for binding various peptides and presenting the peptides to T cells. The formation of a stable peptide−MHC II−TCR complex seems to be necessary for T cell activation (*26*). On the other hand, differences in the dissociation rates are observed among antigen peptides; e.g., the kinetic measurements for the interaction between TCR and APLs showed that the dissociation rate of the antagonist APL was greater than that of the agonist APL (*11*, *12*). However, some ambiguity when T cell activation is explained in terms of kinetic properties still exists. Our thermodynamic study suggests another possibility that the stability of pMHC II plays an important role in the recognition by T cells. Nelson et al. also reported that the half-life of pMHC II on the antigen-presenting cell surface is one of the factors influencing TCR recognition (*27*). The stability of pMHC II would affect not only the frequency of formation of a pMHC II complex on antigen-presenting cells but also the establishment of the peptide−MHC II−TCR complex.

ACKNOWLEDGMENT

We thank Dr. Hatsuho Uedaira at RIKEN for valuable discussions about thermodynamics and technical advice regarding DSC measurements.

REFERENCES

1. Davis, M. M., Boniface, J. J., Reich, Z., Lyons, D., Hampl, J., Arden, B., and Chien, Y. (1998) Ligand recognition by $\alpha\beta$ T cell receptors, *Annu. Rev. Immunol. 16*, 523−544.
2. Cresswell, P. (1994) Assembly, transport, and function of MHC class II molecules, *Annu. Rev. Immunol. 12*, 259−293.
3. Engelhard, V. H. (1994) Structure of peptides associated with class I and class II MHC molecules, *Annu. Rev. Immunol. 12*, 181−207.
4. Sloan-Lancaster, J., and Allen, P. M. (1996) Altered peptide ligand-induced partial T cell activation: molecular mechanisms and role in T cell biology, *Annu. Rev. Immunol. 14*, 1−27.
5. Evavold, B. D., and Allen, P. M. (1991) Separation of IL-4 production from Th cell proliferation by an altered T cell receptor ligand, *Science 252*, 1308−1310.
6. Evavold, B. D., Williams, S. G., Hsu, B. L., Buus, S., and Allen, P. M. (1992) Complete dissection of the Hb(64−76) determinant using T helper 1, T helper 2 clones, and T cell hybridomas, *J. Immunol. 148*, 347−353.
7. Fremont, D. H., Hendrickson, W. A., Marrack, P., and Kappler, J. (1996) Structures of an MHC class II molecule with covalently bound single peptides, *Science 272*, 1001−1004.
8. Kersh, G. J., Miley, M. J., Nelson, C. A., Grakoui, A., Horvath, S., Donermeyer, D. L., Kappler, J., Allen, P. M., and Fremont, D. H. (2001) Structural and functional consequences of altering a peptide MHC anchor residue, *J. Immunol. 166*, 3345−3354.
9. Fremont, D. H., Dai, S., Chiang, H., Crawford, F., Marrack, P., and Kappler, J. (2002) Structural basis of cytochrome *c* presentation by IE^k, *J. Exp. Med. 195*, 1043−1052.
10. Marrack, P., Ignatowicz, L., Kappler, J. W., Boymel, J., and Freed, J. H. (1993) Comparison of peptides bound to spleen and thymus class II, *J. Exp. Med. 178*, 2173−2183.
11. Kersh, G. J., Kersh, E. N., Fremont, D. H., and Allen, P. M. (1998) High- and low-potency ligands with similar affinities for the TCR: the importance of kinetics in TCR signaling, *Immunity 9*, 817−826.
12. Matsui, K., Boniface, J. J., Steffner, P., Reay, P. A., and Davis, M. M. (1994) Kinetics of T-cell receptor binding to peptide/I-E^k complexes: correlation of the dissociation rate with T-cell responsiveness, *Proc. Natl. Acad. Sci. U.S.A. 91*, 12862−12866.
13. Oda, M., Kozono, H., Morii, H., and Azuma, T. (2003) Evidence of allosteric conformational changes in the antibody constant region upon antigen binding, *Int. Immunol. 15*, 417−426.
14. Saito, K., Sarai, A., Oda, M., Azuma, T., and Kozono, H. (2003) Thermodynamic analysis of the increased stability of major histocompatibility complex class II molecule I-E^k complexed with an antigenic peptide at an acidic pH, *J. Biol. Chem. 278*, 14732−14738.
15. Sanchez-Ruiz, J. M., Lopez-Lacomba, J. L., Cortijo, M., and Mateo, P. L. (1988) Differential scanning calorimetry of the irreversible thermal denaturation of thermolysin, *Biochemistry 27*, 1648−1652.
16. Kozono, H., Parker, D., White, J., Marrack, P., and Kappler, J. (1995) Multiple binding sites for bacterial superantigens on soluble class II MHC molecules, *Immunity 3*, 187−196.
17. Kozono, H., White, J., Clements, J., Marrack, P., and Kappler, J. (1994) Production of soluble MHC class II proteins with covalently bound single peptides, *Nature 369*, 151−154.
18. Sadegh-Nasseri, S., and Germain, R. N. (1991) A role for peptide in determining MHC class II structure, *Nature 353*, 167−170.
19. Sadegh-Nasseri, S., and Germain, R. N. (1992) How MHC class II molecules work: peptide-dependent completion of protein folding, *Immunol. Today 13*, 43−46.
20. McCrary, B. S., Bedell, J., Edmondson, S. P., and Shriver, J. W. (1998) Linkage of protonation and anion binding to the folding of Sac7d, *J. Mol. Biol. 276*, 203−224.
21. Petrosian, S. A., and Makhatadze, G. I. (2000) Contribution of proton linkage to the thermodynamic stability of the major cold-shock protein of *Escherichia coli* CspA, *Protein Sci. 9*, 387−394.
22. Fauchere, J. L., and Pliska, V. (1983) Hydrophobic parameters π of amino-acid side chains from the partitioning of *N*-acetyl-amino-acid amides, *Eur. J. Med. Chem. 18*, 369−375.
23. Thomas, S. T., Loladze, V. V., and Makhatadze, G. I. (2001) Hydration of the peptide backbone largely defines the thermodynamic propensity scale of residues at the C′ position of the C-capping box of α-helices, *Proc. Natl. Acad. Sci. U.S.A. 98*, 10670−10675.
24. Belmares, M. P., Rabinowitz, J. D., Liu, W., Mellins, E. D., and McConnell, H. M. (2000) pH stability of HLA-DR4 complexes with antigenic peptides, *Biochemistry 39*, 14558−14566.
25. Schmitt, L., Boniface, J. J., Davis, M. M., and McConnell, H. M. (1998) Kinetic isomers of a class II MHC-peptide complex, *Biochemistry 37*, 17371−17380.
26. Bromley, S. K., Burack, W. R., Johnson, K. G., Somersalo, K., Sims, T. N., Sumen, C., Davis, M. M., Shaw, A. S., Allen, P. M., and Dustin, M. L. (2001) The immunological synapse, *Annu. Rev. Immunol. 19*, 375−396.
27. Nelson, C. A., Petzold, S. J., and Unanue, E. R. (1994) Peptides determine the lifespan of MHC class II molecules in the antigen-presenting cell, *Nature 371*, 250−252.

BI049838F